Advances in Nano Research, *Vol. 9, No. 2 (2020) 105-112*
DOI: https://doi.org/10.12989/anr.2020.9.2.105

Two-dimensional modelling of uniformly doped silicene with aluminium and its electronic properties

M.W. Chuan, K.L. Wong, A. Hamzah, S. Rusli, N.E. Alias, C.S. Lim and M.L.P. Tan*

School of Electrical Engineering, Faculty of Engineering, Universiti Teknologi Malaysia, 81310 Skudai, Johor, Malaysia

(*Received February 28, 2020, Revised July 24, 2020, Accepted July 28, 2020*)

Abstract. Silicene is a two-dimensional (2D) derivative of silicon (Si) arranged in honeycomb lattice. It is predicted to be compatible with the present fabrication technology. However, its gapless properties (neglecting the spin-orbiting effect) hinders its application as digital switching devices. Thus, a suitable band gap engineering technique is required. In the present work, the band structure and density of states of uniformly doped silicene are obtained using the nearest neighbour tight-binding (NNTB) model. The results show that uniform substitutional doping using aluminium (Al) has successfully induced band gap in silicene. The band structures of the presented model are in good agreement with published results in terms of the valence band and conduction band. The band gap values extracted from the presented models are 0.39 eV and 0.78 eV for uniformly doped silicene with Al at the doping concentration of 12.5% and 25% respectively. The results show that the engineered band gap values are within the range for electronic switching applications. The conclusions of this study envisage that the uniformly doped silicene with Al can be further explored and applied in the future nanoelectronic devices.

Keywords: 2D material; doped silicene; band structure; density of states; band gap engineering

1. Introduction

Moore's law is approaching its end as transistors are scaled to sub-10 nanometers regime that features less than tens of atoms in a device (Waldrop 2016). This constraint has urged the research efforts in discovering potential candidates for "more than Moore's" nanoelectronic devices (Ye *et al*. 2019, Chuan *et al*. 2020). One of the ground-breaking developments is the success of graphene synthesis (Novoselov *et al*. 2004). Interestingly, the researchers who have discovered graphene were awarded the Nobel Prize. Due to its extraordinary electronic and mechanical properties, graphene has attracted rigorous attentions among researchers (Najam *et al*. 2016, Rodriguez-Perez *et al*. 2017, Low and Shon 2018, Xue *et al*. 2019). The graphene fabrication technology is still in its infancy level: large area production with good electrical properties and affordable production cost has not yet been reported (Ferrari *et al*. 2015).

Driven by the success of graphene, other two-dimensional (2D) materials such as transition metal dichalcogenides (TMDs) (Wang *et al*. 2012, 2019), hexagonal boron nitride (h-BN) (Golberg *et al*. 2010, Lim *et al*. 2018), phosphorene (Carvalho *et al*. 2016, Menezes and Capaz 2018, Watts *et al*. 2019) and silicene (Zhang *et al*. 2014, Molle *et al*. 2018, Chuan *et al*. 2020) are extensively studied. Akinwande *et al*. (2019) have identified that 2D materials face major challenges in terms of their compatibility with silicon (Si) complementary metal-oxide-semiconductor (CMOS) technology (Akinwande *et al*. 2019). Interestingly, silicene is the monolayer allotrope of Si arranged in honeycomb lattice structure which shares similar electronic properties with graphene, and yet acquires added advantage due to its compatibility with Si wafer technology (Tao *et al*. 2015). This is crucial as the Si technology is well understood and established in the semiconductor industry. An overview of silicene-related research is discussed in the next section.

2. Related research

Nanosheet field-effect transistors (FETs) using thin sheets of Si can be the last possible step for transistor scaling (Ye *et al*. 2019). However, similar to pristine graphene, pristine silicene has almost zero band gap (neglecting spin-orbiting effect) at the Dirac point from the band structure, which inhibits its potential as FETs. In 1994, Takeda and Shiraishi (Takeda and Shiraishi 1994) have predicted the existence of Si monolayer structure theoretically using first-principles calculations. This early theoretical prediction of monolayer silicene was further stimulated by the success of mechanically-exfoliated graphene discovery in 2004 (Zhao *et al*. 2016, Chuan *et al*. 2020).

The findings of Takeda and Shiraishi (1994) were later extended by other theoretical works based on first-principles calculations (Durgun *et al*. 2005, Yang and Ni 2005), density functional theory (DFT) (Cahangirov *et al*. 2009, Ding and Ni 2009) and tight-binding (TB) approach (Guzmán-Verri and Voon 2007).

*Corresponding author, Ph.D.,
E-mail: michael@utm.my

ISSN: 2287-237X (Print), 2287-2388 (Online)

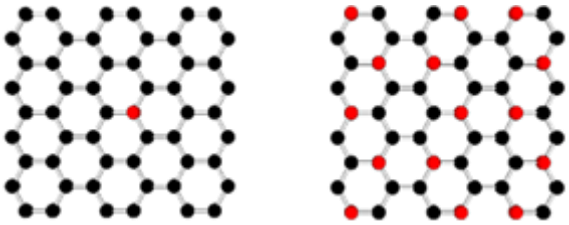

(a) (b)

Fig. 1 Schematic diagram of (a) selective single doping and (b) uniform doping where black and red atoms represent the original and the dopant atoms respectively

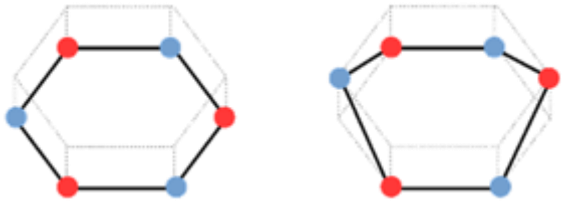

(a) (b)

Fig. 2 Schematic diagram of (a) planar hexagonal and (b) boat-like lattice structures (Ding and Wang 2013)

Their results have confirmed that pristine silicene is a semi-metallic material possessing a Dirac cone at the *K*-point in the first Brillouin zone (FBZ). As a result, silicene has extremely high charge carrier mobility due to the massless fermions (Novoselov *et al*. 2005).

In recent years, the amount of literature on silicene incorporating various band gap engineering techniques are increasing (Zhao *et al*. 2016). For instances, the introduction of defects (Song *et al*. 2011, Iordanidou *et al*. 2016, Ali *et al*. 2017), substitutional doping (Ding and Wang 2013, Chen *et al*. 2014, Lopez-Bezanilla 2014, Jiang *et al*. 2018), strain engineering (Liu *et al*. 2012, Qin *et al*. 2012, Yang *et al*. 2014) and many other techniques are extensively explored. Among these studies, substitutional doping is found to be an effective approach to induce band gap in silicene. The common dopants are boron (B), aluminium (Al), nitrogen (N) and phosphorus (P). The results shown by Chen *et al*. (2014) and Jiang *et al*. (2018) suggest that the electronic properties of doped silicene using single or double atom substitutional doping technique is dependent on the doping sites. In contrast, the DFT study conducted by Ding and Wang (2013) have discovered useful band gap values in uniformly doped silicene sheets (known as SiX and XSi_3 sheets in their paper). In addition, the electronic properties of uniformly doped structures are independent on the dopant sites. The difference between the two doping techniques are shown in Fig. 1.

Although doping silicene uniformly with either Al or P can both induce semiconducting band gaps, Al has been chosen in this work because this dopant can retain the stable planar hexagonal lattice structure of silicene (Ding and Wang 2013) as depicted in Fig. 2(a). On the other hand, doping silicene uniformly with P would produce the boat-like stable structure as shown in Fig. 2(b). The fitting parameters of nearest neighbour tight-binding (NNTB) model has been computed by benchmarking with published result. After verifying the accuracy of the fitting parameters using root mean square deviation (RMSD), the modelling work is further extended by reducing the doping concentration of the Al atoms from 25% (2 dopant atoms out of 8 atoms) to 12.5% (1 dopant atom out of 8 atoms).

The rest of the paper is organised as follows. Section 3 presents the computation of NNTB model for the electronic properties of uniformly doped silicene monolayers with Al in terms of the band structure and density of states (DOS) by solving the time-independent Schrödinger equation. Subsequently, Section 4 describes and discusses the main findings of NNTB model for the uniformly doped silicene with Al: the band structures, band gap values, and DOS. The conclusion and future recommendation of this study are reported in Section 5.

3. Mathematical modelling

The modelling procedures and equations used for the electronic properties of pristine silicene and uniformly doped silicene are described in details in this section.

3.1 Modelling of band structure and density of states

The schematic diagram of the pristine and uniformly doped silicene are shown in Fig. 3. The band structures of the 2D sheets are modelled using the NNTB model based on the time-independent Schrödinger equation (Datta 2005, Chuan *et al*. 2020), expressed as

$$E(\emptyset_0) = \left[h(\vec{k})\right](\emptyset_0) \tag{1}$$

where E is the total energy, $\emptyset_0$ is the wave function and $[h(\vec{k})]$ is the matrix equation given by Eq. (2).

$$\left[h(\vec{k})\right] = \sum_{m=1,n}^{4} H_{nm} e^{i\vec{k}(\vec{r}_n - \vec{r}_m)} \tag{2}$$

where H_{nm} is the Hamiltonian matrix equation, $\vec{k}$ is the wave vector, $\vec{r}_n$ and $\vec{r}_m$ are the position vectors which describe the displacement of m^{th} unit cell with respect to the n^{th} unit cell. The origin is placed at one of the atoms of the n^{th} unit cell. The interactions between the unit cells within the nearest neighbours are obtained by expanding Eq. (2) to obtain Eq. (3), given as

$$\begin{aligned}\left[h(\vec{k})\right] = {} & H_{nn} + H_{n1} e^{i\vec{k}(\vec{r}_n - \vec{r}_1)} + H_{n2} e^{i\vec{k}(\vec{r}_n - \vec{r}_2)} \\ & + H_{n3} e^{i\vec{k}(\vec{r}_n - \vec{r}_3)} + H_{n4} e^{i\vec{k}(\vec{r}_n - \vec{r}_4)}\end{aligned} \tag{3}$$

The energy eigenstates for energy momentum dispersion and $E(k)$ relation are generated by using the standard solution for eigenvalue problem, given by

$$\det\left|\left[h(\vec{k})\right] - EI\right| = 0 \tag{4}$$

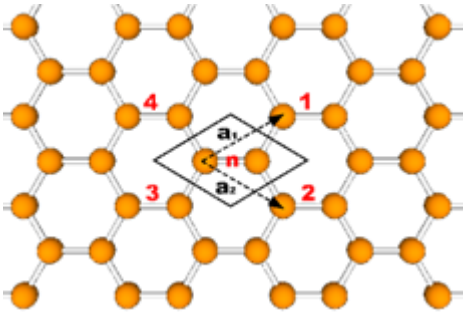

(a)

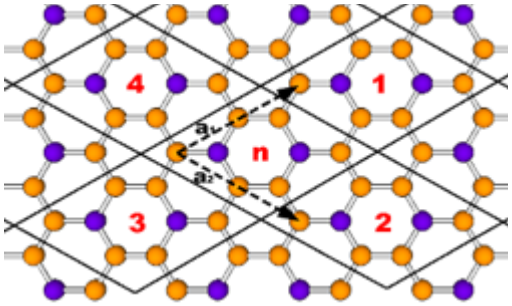

(b)

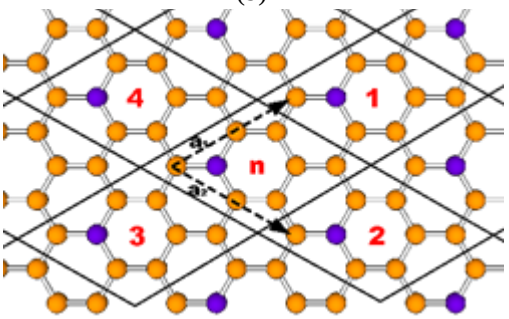

(c)

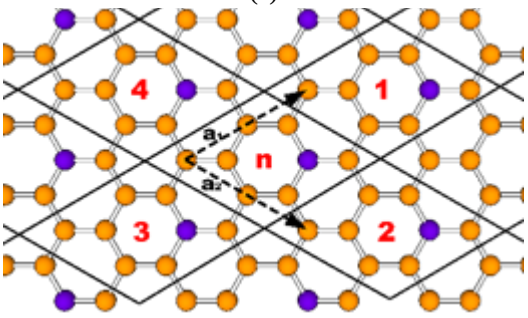

(d)

Fig. 3 Schematic diagram of (a) pristine silicene, (b)-(d) uniformly doped silicene monolayers where orange and purple atoms represent Si and Al atoms respectively, a_1 and a_2 are the displacement vectors and the black rhombuses are primitive unit cells. The bold red numbers denote the n^{th} unit cell and its four nearest neighbours

where I is the identity matrix of the same size as $[h(\vec{k})]$. The size of the matrices depends on the number of atoms in a unit cell, where the size is 2 X 2 and 8 X 8 for pristine and uniformly doped silicene respectively.

DOS describes the electronic properties in term of the number of available states in a system. The DOS is

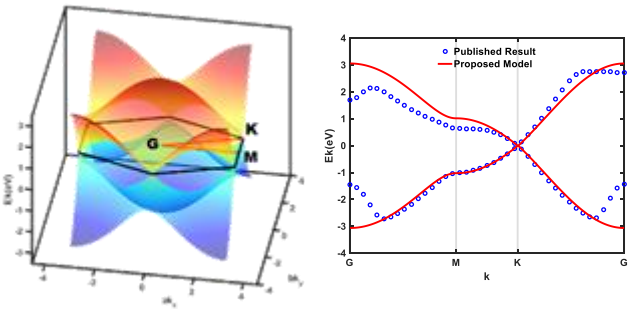

(a) (b)

Fig. 4 Band structure of pristine silicene (a) in three-dimensional (3D) plot and (b) in 2D plot within the FBZ. Blue dotted line is adapted from Shao *et al*. (2013) for benchmarking and red line is the result of present model

computed numerically using the solution of delta (δ) function (Datta 2005), expressed as

$$\mathrm{DOS}(E) = \sum_{i=1}^{N} \frac{1}{2\pi} \sum_{all\ k} \frac{2\eta}{[E - \varepsilon(k)]^2 + \eta^2} \tag{5}$$

where $\varepsilon(k)$ is the energy eigenstate, E is the energy value as it is iterated from the minimum value of $E(k)$ to maximum value of $\varepsilon(k)$ and η is a very small value to prevent the inverse matrix from diverging. In this paper, the schematic structures in Fig. 3 are assumed to be planar with regular hexagonal lattice arrangement (120° per interior angle).

3.2 Hamiltonian matrix and tight-binding parameter

Using Eq. (3), the Hamiltonian matrices for the silicene structures can be obtained. The Hamiltonian matrix for pristine silicene is derived based on Fig. 3(a), and is given by

$$[h(\vec{k})]_{pristine} = \begin{bmatrix} E_{oSi} & h_0 \\ h_0^{*} & E_{oSi} \end{bmatrix} \tag{6}$$

where E_{oSi} is the on-site energy for Si atom (is assumed to be $0\ eV$ for pristine silicene for simplification), $h_0 = 2t_{Si-Si}e^{-iak_x}\cos(bk_y)$ and $h_0{}^{*}$ is the complex conjugate of h_0. In the h_0 expression, t_{Si-Si} is the hopping integral for Si-Si atoms; k_x and k_y are the x- and y-components of the wave vectors; a and b are the x- and y-components of the displacement vectors. By solving Eq. (6) using Eq. (4), the simplified analytical dispersion relation of pristine silicene is given as

$$E(\vec{k})_{pristine} = \pm t_{Si-Si}\sqrt{3 + 2\cos(2bk_y) + 4\cos(ak_x)\cos(bk_y)} \tag{7}$$

Figs. 4(a)-(b) depict the band structure of pristine silicene plotted using Eq. (7) in three-dimensional (3D) and

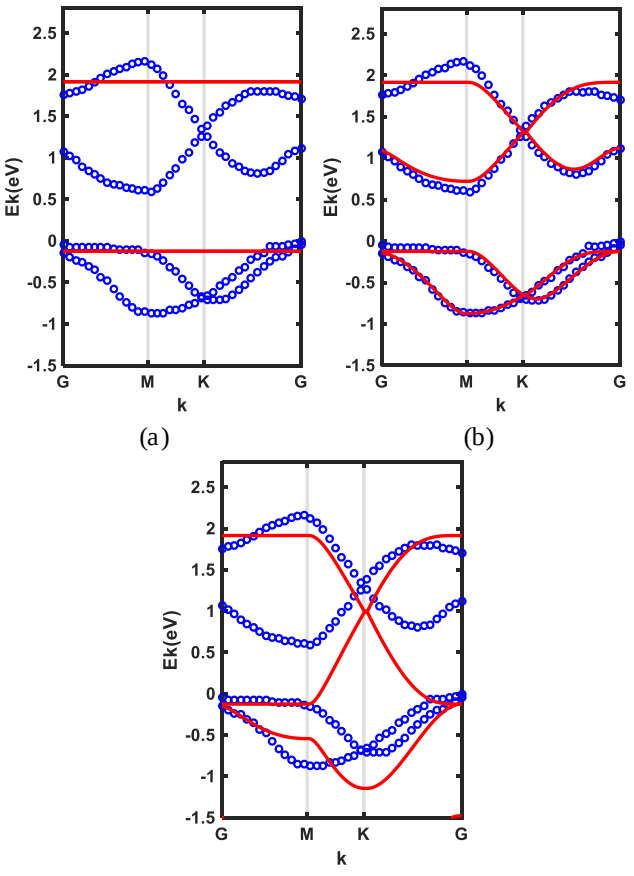

Fig. 5 Band structures of $AlSi_3$ within the FBZ by manipulating the values of hopping integral, t_{Al-Si} at (a) 0 eV, (b) -1.0 eV and (c) -2.5 eV, respectively. Blue dotted lines are adapted from Ding and Wang (2013) and red solid line is NNTB band structure of present model with varying t_{Al-Si}

2D plot respectively. In previous studies, the proposed t_{Si-Si} is -1.60 eV (Liu *et al*. 2011) and -1.03 eV (Roome and Carey 2014). However, the t_{Si-Si} used in this paper is -1.02 eV by benchmarking with the results from first-principle calculation by Shao *et al*. (2013). Since the hopping integral is generally obtained by fitting the parameter to the experimental or complex computational results, this parameter may vary accordingly (Lim *et al*. 2017). The obtained band structure agrees with published results (Guzmán-Verri and Voon 2007, Cahangirov *et al*. 2009, Shao *et al*. 2013), showing that pristine silicene is a gapless material.

The same modelling procedure based on Eq. (3) is repeated to obtain the Hamiltonian matrices for uniformly doped silicene with Al as shown Figs. 3(b), (c) and (d). Fig. 3(b) shows the schematic diagram of unifomly doped silicene with 25% concentration of Al atoms while Figs. 3(c) and (d) show the schematic diagrams of uniformly doped silicene with 12.5% concentration of Al atoms. The difference between Figs. 3(c) and (d) are the dopants locations of the Al atoms in the primitive unit cell, that is, left and right oriented respectively.

To simplify the description of the uniformly doped silicene structures in this paper, the structures shown in Figs. 3(b), (c) and (d) will be referred as $AlSi_3$, $AlSi_{7L}$ and $AlSi_{7R}$ respectively, hereafter. The models with the same doping concentration of 12.5% Al atoms namely, $AlSi_{7L}$ and $AlSi_{7R}$, are constructed to study the effects of doping concentration and orientation of Al on the electronic properties of silicene. The derived Hamiltonian matrices are shown in Eqs. (8), (9) and (10) for the 2D structures as depicted in Figs. 3(b), (c) and (d) respectively.

$$[h(\vec{k})]_{AlSi_3} = \begin{bmatrix} E_{oSi} & 0 & 0 & \boldsymbol{t_{Al-Si}} & 0 & h_1 & h_2 & 0 \\ 0 & E_{oSi} & 0 & \boldsymbol{t_{Al-Si}} & 0 & 0 & t_{Si-Si} & h_1 \\ 0 & 0 & E_{oSi} & \boldsymbol{t_{Al-Si}} & 0 & t_{Si-Si} & 0 & h_2 \\ \boldsymbol{t_{Al-Si}} & \boldsymbol{t_{Al-Si}} & \boldsymbol{t_{Al-Si}} & \boldsymbol{E_{oAl}} & 0 & 0 & 0 & 0 \\ 0 & 0 & 0 & 0 & \boldsymbol{E_{oAl}} & \boldsymbol{t_{Al-Si}} & \boldsymbol{t_{Al-Si}} & \boldsymbol{t_{Al-Si}} \\ h_1^* & 0 & t_{Si-Si} & 0 & \boldsymbol{t_{Al-Si}} & E_{oSi} & 0 & 0 \\ h_2^* & t_{Si-Si} & 0 & 0 & \boldsymbol{t_{Al-Si}} & 0 & E_{oSi} & 0 \\ 0 & h_1^* & h_2^* & 0 & \boldsymbol{t_{Al-Si}} & 0 & 0 & E_{oSi} \end{bmatrix} \quad (8)$$

$$[h(\vec{k})]_{AlSi_{7L}} = \begin{bmatrix} E_{oSi} & 0 & 0 & \boldsymbol{t_{Al-Si}} & 0 & h_1 & h_2 & 0 \\ 0 & E_{oSi} & 0 & \boldsymbol{t_{Al-Si}} & 0 & 0 & t_{Si-Si} & h_1 \\ 0 & 0 & E_{oSi} & \boldsymbol{t_{Al-Si}} & 0 & t_{Si-Si} & 0 & h_2 \\ \boldsymbol{t_{Al-Si}} & \boldsymbol{t_{Al-Si}} & \boldsymbol{t_{Al-Si}} & \boldsymbol{E_{oAl}} & 0 & 0 & 0 & 0 \\ 0 & 0 & 0 & 0 & E_{oSi} & t_{Si-Si} & t_{Si-Si} & t_{Si-Si} \\ h_1^* & 0 & t_{Si-Si} & 0 & t_{Si-Si} & E_{oSi} & 0 & 0 \\ h_2^* & t_{Si-Si} & 0 & 0 & t_{Si-Si} & 0 & E_{oSi} & 0 \\ 0 & h_1^* & h_2^* & 0 & t_{Si-Si} & 0 & 0 & E_{oSi} \end{bmatrix} \quad (9)$$

$$[h(\vec{k})]_{AlSi_{7R}} = \begin{bmatrix} E_{oSi} & 0 & 0 & t_{Si-Si} & 0 & h_1 & h_2 & 0 \\ 0 & E_{oSi} & 0 & t_{Si-Si} & 0 & 0 & t_{Si-Si} & h_1 \\ 0 & 0 & E_{oSi} & t_{Si-Si} & 0 & t_{Si-Si} & 0 & h_2 \\ t_{Si-Si} & t_{Si-Si} & t_{Si-Si} & E_{oSi} & 0 & 0 & 0 & 0 \\ 0 & 0 & 0 & 0 & \boldsymbol{E_{oAl}} & \boldsymbol{t_{Al-Si}} & \boldsymbol{t_{Al-Si}} & \boldsymbol{t_{Al-Si}} \\ h_1^* & 0 & t_{Si-Si} & 0 & \boldsymbol{t_{Al-Si}} & E_{oSi} & 0 & 0 \\ h_2^* & t_{Si-Si} & 0 & 0 & \boldsymbol{t_{Al-Si}} & 0 & E_{oSi} & 0 \\ 0 & h_1^* & h_2^* & 0 & \boldsymbol{t_{Al-Si}} & 0 & 0 & E_{oSi} \end{bmatrix} \quad (10)$$

Eqs. (8), (9) and (10) are the Hamiltonian matrices, $[h(\vec{k})]$ for $AlSi_3$, $AlSi_{7L}$ and $AlSi_{7R}$ respectively. E_{oAl} is the on-site energy for Al atom, $t_{Al-Si} = t_{Si-Al}$ is the hopping integral for Al-Si (or Si-Al) atoms, $h_1 = t_{Si-Si}e^{-i(ak_x - bk_y)}$ and $h_2 = t_{Si-Si}e^{-i(ak_x + bk_y)}$. Similarly, h_1^* and h_2^* are the complex conjugate of h_1 and h_2 respectively. The TB parameters that are caused by substitution of the Al atoms to the Si atoms are highlighted in bold red font in the Hamiltonian matrices. Subsequently, Eqs. (8), (9) and (10) are solved using Eq. (4) to obtain the band structures. The solutions for an 8 X 8 matrix eigenvalue problem are generally eighth order polynomial characteristic equations, that is, practically not useful to be written. As such, the energy eigenstates for unifomly doped silicene are computed numerically to plot the band structures.

Eq. (8) is solved and fitted to published results adapted from (Ding and Wang 2013) to obtain the tight-binding parameters. The hopping integral, t_{Si-Si} is fixed at -1.02 eV, same as the previously obtained value for the pristine silicene model. The on-site energies, E_{oSi} and E_{oAl} are adapted from (Harrison 2004) where only the p-

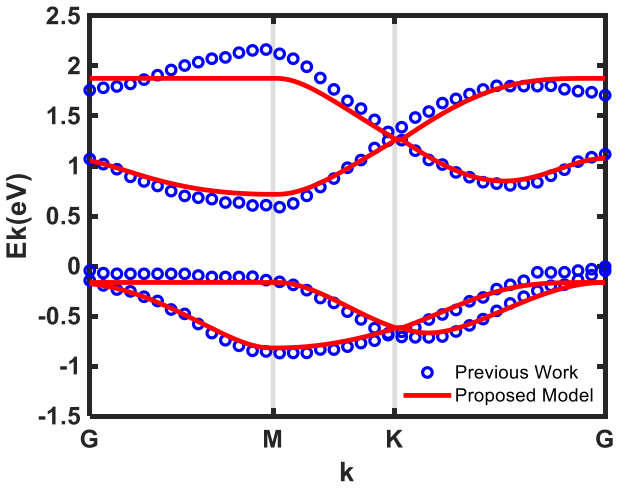

(a)

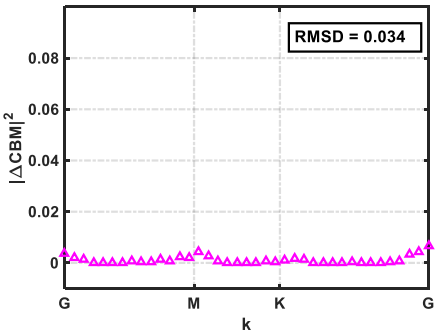

(b)

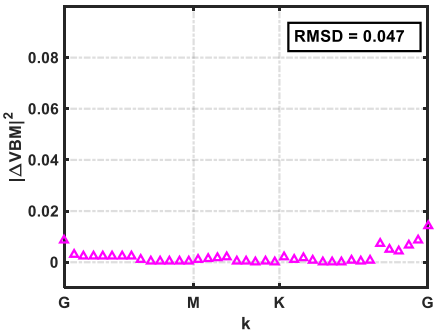

(c)

Fig. 6 (a) Band structure of $AlSi_3$ for the FBZ. The blue dotted curve is adapted from Ding and Wang (2013). The squared difference between proposed model and published result for (b) conduction band minimum (CBM) and (c) valence band maximum (VBM)

orbital energies are considered in this work. To obtain the missing hopping parameter for Al-Si (or Si-Al) atoms, the relationship between t_{Al-Si} and the band structure is examined. In this work, the Fermi level is assumed to be 0 eV. Fig. 5 clearly shows that the band structures are distorted when incorrect values are chosen. At zero t_{Al-Si} value, the energy bands are just straight lines; the slope of the energy bands increases as the magnitude of $|t_{Al-Si}|$ increases.

After adjusting the parameters accordingly, we fitted the NNTB model to the results of the published results from Ding and Wang (2013). Fig. 6(a) shows the optimised results by using fitting procedures as shown in Figs. 5(a), (b) and (c) to determine the fitting parameters. The NNTB model is not capable to completely reproduce the band structure from DFT calculation, but it can be used to fit two important energy bands: the conduction band and the valence band. Conduction band and valence band are sufficient to describe the carrier transports in most of the semiconductor devices. Moreover, the TB approximation is suitable for describing the non-metallic materials with less computational cost compared to sophisticated computational software (LeSar 2013) and the results are useful for further explorations. The obtained parameters from the fitting procedure to plot the correct band structure in Fig. 6(a) is summarised in Table 1.

Table 1 The computed NNTB model parameters for uniformly doped silicene

Parameters	t_{Si-Si}	t_{Al-Si}	E_{oSi}	E_{oAl}
Values (eV)	-1.02	-1.05	-7.59	-5.71

The performance of the proposed model is evaluated by using RMSD. RMSD is a statistical approach that helps to provide a complete evaluation of the error distribution of a model (Chai and Draxler 2014, Leong *et al*. 2020), given by

$$RMSD = \sqrt{\frac{1}{N}\sum_{i=1}^{N} {e_i}^2} \tag{11}$$

where N is the total number of data, e_i is the error at i^{th} data. In this paper, e_i is the difference between the i^{th} data of published result and i^{th} data of proposed model, given as

$$e_i = |\Delta CBM_i| = \left|CBM_{i(published)} - CBM_{i(proposed)}\right| \tag{12}$$

$$e_i = |\Delta VBM_i| = |VBM_{i\,(published)} - VBM_{i(proposed)}| \tag{13}$$

Eqs. (12) and (13) are used to obtain the errors of i^{th} data for CBM and VBM respectively and the squared values of the error are plotted in Figs. 6(b) and (c). The calculated RMSDs are 0.034 for CBM and 0.047 for VBM. These close-to-zero RMSD values indicate that the proposed model is consistent with published result.

4. Results and discussion

4.1 Band structures and density of states

The computed band structures and DOS for $AlSi_3$ model based on the solution of Hamiltonian matrix expressed in Eq. (8) is shown in Fig. 7. The doping concentration for this structure is 25% where there are 2 Al atoms and 6 Si atoms in each unit cell. The band gap, E_g of the structure can be obtained using

$$E_g = |CBM - VBM| \tag{13}$$

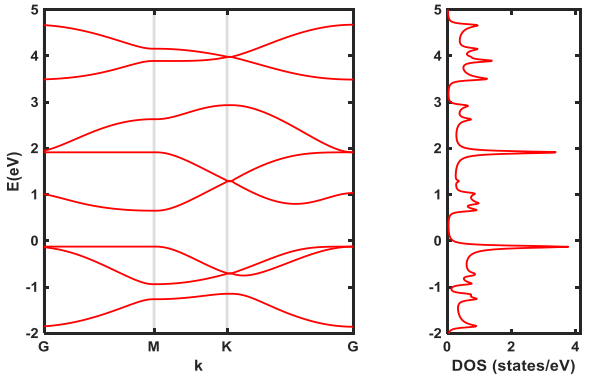

(a) (b)

Fig. 7 Plots of (a) band structure and (b) DOS for $AlSi_3$

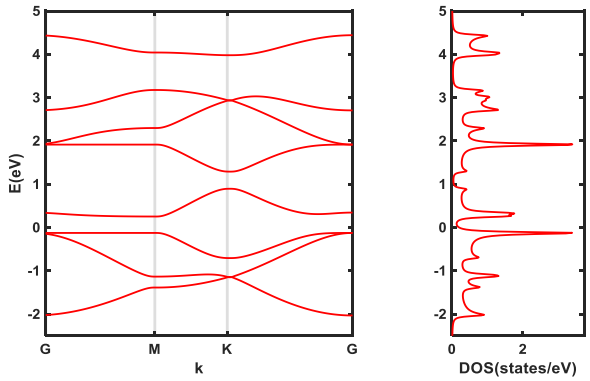

(a) (b)

Fig. 8 Plots of (a) band structure and (b) DOS for $AlSi_7$

The CBM and VBM extracted from the band structure of $AlSi_3$ is 0.64 eV and -0.13 eV respectively. By applying Eq. (14), the extracted band gap for $AlSi_3$ is 0.78eV.

Fig. 8 depicts the computed band structures and DOS for $AlSi_{7L}$ and $AlSi_{7R}$ models based on Eqs. (9) and (10). The doping concentration for this structure is 12.5% where there are 1 Al atom and 7 Si atoms in each unit cell. Although two different orientations of doping ($AlSi_{7L}$ and $AlSi_{7R}$) are considered, the results show no difference in their band structure and DOS. Therefore, only one of the results is shown. The CBM and VBM extracted from the band structure of $AlSi_{7L/R}$ is 0.26 eV and -0.13 eV, respectively which represents a band gap of 0.39 eV. The band gap value of $AlSi_{7L/R}$ is half of the band gap value of $AlSi_3$.

4.2 Discussion on the proposed models

The comparisons of the proposed models are indicated in Figs. 9(a) and (b). It is clearly shown that the induced band gap of the silicene has become larger as the doping concentration of Al is increased from 0% to 25% in Fig. 9(a). These promising results show that the extracted band gap values are suitable for the applications in the areas of nanoelectronics (based on the standard value of band gap which is between 0.1 eV (Ni *et al*. 2014) and 3 eV (Lim *et al*. 2017). The band gap values for $AlSi_3$ and $AlSi_7$ are also

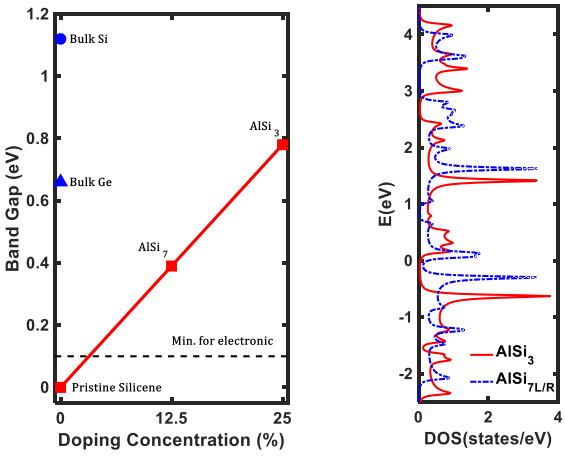

(a) (b)

Fig. 9 Graphs of (a) the relationship between doping concentration and band gap, (b) DOS of $AlSi_3$ and $AlSi_7$ in the same plot

comparable to bulk Si (1.12 eV) and Ge (0.66 eV). In addition, it is found that the doping concentration changes the DOS of the uniformly doped silicene sheets as shown in Fig. 9(b). It is observed that the peaks in the DOS, which are also known as Van Hove singularities (Lim *et al*. 2018), have shifted upwards when the doping concentration is decreased from 25% to 12.5%. However, the computations of the carrier transport properties and the current-voltage characteristics are required to examine the significant impacts of the DOS to the device performance of the materials (Arora 2015).

In summary, the band structures and DOS of pristine silicene and uniformly doped silicene can be modelled using the NNTB approach. However, this approach requires fitting procedures to obtain the tight-binding parameters and it is unable to describe the stability of the lattice. Despite the mentioned drawbacks, this work has successfully described the fundamental electronic properties of the silicene structures. These results provide opportunity for further investigations such as applying non-equilibrium conditions to the models (Datta 2000, Wong *et al*. 2020). Besides, further studies can be conducted to analyse the carrier transport properties of the materials before proceeding to modelling and simulation at the device level. Alternatively, this study can also be extended by employing dislocations and defects in the perfect crystalline structures, which can greatly alter the electronic properties of the nanostructures (Mehdi Aghaei and Calizo 2015, Wong *et al*. 2019, Chuan *et al*. 2020).

5. Conclusions

The electronic properties in terms of the band structure and DOS of uniformly doped silicene with Al have been modelled using the NNTB approach. The hopping integral for the interaction between Al and Si atoms has also been computed by validation with published DFT calculations. In addition, the results of developed models are in good agreement with published results. The relationship between

the doping concentrations of Al atoms to the band structure of silicene is also discussed. When the doping concentration of Al atoms in the silicene sheet increases, the band gap of the material increases. Moreover, it is noted that the left- and right- oriented $AlSi_7$ sheets produce the same results although the Hamiltonian matrices for these structures are different. The band gap of silicene has been successfully engineered using substitutional doping with Al at uniform concentrations. The uniformly doped silicene has potential in nanoelectronic applications, namely digital switching devices. Further studies are recommended to predict the carrier transport properties and current-voltage characteristics of the uniformly doped silicene sheets at non-equilibrium conditions.

Acknowledgments

The authors acknowledge the Research Management Centre (RMC) of Universiti Teknologi Malaysia (UTM) for providing excellent support and conducive research environment. Mu Wen expresses his appreciation for the award of PhD Zamalah Scholarship from the School of Graduate Studies, UTM. Michael Tan would like to acknowledge the financial support from UTM Fundamental Research (UTMFR) (Vote No. Q.J130000.2551.21H51) that allowed the research to proceed smoothly.

References

Akinwande, D., Huyghebaert, C., Wang, C.H., Serna, M.I., Goossens, S., Li, L.J., Wong, H.S.P. and Koppens, F.H. (2019), "Graphene and two-dimensional materials for silicon technology", *Nature*, **573**(7775), 507-518. https://doi.org/10.1038/s41586-019-1573-9.

Ali, M., Pi, X., Liu, Y. and Yang, D. (2017), "Electronic and magnetic properties of graphene, silicene and germanene with varying vacancy concentration", *AIP Adv.*, **7**(4), 045308. https://doi.org/10.1063/1.4980836.

Arora, V.K. (2015), *Nanoelectronics: Quantum Engineering of Low-Dimensional Nanoensembles*, CRC Press, USA. https://doi.org/10.1201/b18131.

Cahangirov, S., Topsakal, M., Aktürk, E., Şahin, H. and Ciraci, S. (2009), "Two-and one-dimensional honeycomb structures of silicon and germanium", *Phys. Rev. Lett.*, **102**(23), 236804. https://doi.org/10.1103/PhysRevLett.102.236804.

Carvalho, A., Wang, M., Zhu, X., Rodin, A.S., Su, H. and Neto, A.H.C. (2016), "Phosphorene: from theory to applications", *Nat. Rev. Mater.*, **1**(11), 16061. https://doi.org/10.1038/natrevmats.2016.61.

Chai, T. and Draxler, R.R. (2014), "Root mean square error (RMSE) or mean absolute error (MAE)? - arguments against avoiding RMSE in the literature", *Geosci. Model Dev.*, **7**(3), 1247-1250. https://doi.org/10.5194/gmd-7-1247-2014.

Chen, J., Wang, X.F., Vasilopoulos, P., Chen, A.B. and Wu, J.C. (2014), "Single and multiple doping effects on charge transport in zigzag silicene nanoribbons", *Chemphyschem*, **15**(13), 2701-2706. https://doi.org/10.1002/cphc.201402171.

Chuan, M.W., Wong, K.L., Hamzah, A., Alias, N.E., Lim, C.S. and Tan, M.L.P. (2020), "Electronic properties of zigzag silicene nanoribbons with single vacancy defect", *Indones. J. Electr. Eng. Comput. Sci.*, **19**(1), 76-84. http://doi.org/10.11591/ijeecs.v19.i1.pp76-84.

Chuan, M.W., Wong, K.L., Hamzah, A., Rusli, S., Alias, N.E., Lim, C.S. and Tan, M.L.P. (2020) "2D honeycomb silicon: a review on theoretical advances for silicene field-effect transistors", *Curr. Nanosci.*, **16**(4), 595-607. https://doi.org/10.2174/1573413715666190709120019.

Chuan, M.W., Wong, K.L., Hamzah, A., Rusli, S., Alias, N.E., Lim, C.S. and Tan, M.L.P. (2020) "Electronic properties and carrier transport properties of low-dimensional aluminium doped silicene nanostructure", *Physica E Low Dimens. Syst. Nanostruct.*, **116**, 113731. https://doi.org/10.1016/j.physe.2019.113731.

Chuan, M.W., Wong, K.L., Hamzah, A., Rusli, S., Alias, N.E., Lim, C.S. and Tan, M.L.P. (2020) "A review of the top of the barrier nanotransistor models for semiconductor nanomaterials", *Superlattices Microstruct.*, **140**, 106429. https://doi.org/10.1016/j.spmi.2020.106429.

Datta, S. (2000), "Nanoscale device modeling: the Green's function method", *Superlattices Microstruct.*, **28**(4), 253-278. https://doi.org/10.1006/spmi.2000.0920.

Datta, S. (2005), *Quantum Transport: Atom to Transistor*, Cambridge University Press, UK. https://doi.org/10.1017/CBO9781139164313.

Ding, Y. and Ni, J. (2009), "Electronic structures of silicon nanoribbons", *Appl. Phys. Lett.*, **95**(8), 083115. https://doi.org/10.1063/1.3211968.

Ding, Y. and Wang, Y. (2013), "Density functional theory study of the silicene-like SiX and XSi_3 (X = B, C, N, Al, P) honeycomb lattices: The various buckled structures and versatile electronic properties", *J. Phys. Chem. C*, **117**(35), 18266-18278. https://doi.org/10.1021/jp407666m.

Durgun, E., Tongay, S. and Ciraci, S. (2005), "Silicon and III-V compound nanotubes: structural and electronic properties", *Phys. Rev. B*, **72**(7), 075420. https://doi.org/10.1103/PhysRevB.72.075420.

Ferrari, A.C., Bonaccorso, F., Fal'Ko, V., Novoselov, K.S., Roche, S., Bøggild, P., Borini, S., Koppens, F.H., Palermo, V. and Pugno, N. (2015), "Science and technology roadmap for graphene, related two-dimensional crystals, and hybrid systems", *Nanoscale*, **7**(11), 4598-4810. https://doi.org/10.1039/c4nr01600a.

Golberg, D., Bando, Y., Huang, Y., Terao, T., Mitome, M., Tang, C. and Zhi, C. (2010), "Boron nitride nanotubes and nanosheets", *ACS Nano*, **4**(6), 2979-2993. https://doi.org/10.1021/nn1006495.

Guzmán-Verri, G.G. and Voon, L.L.Y. (2007), "Electronic structure of silicon-based nanostructures", *Phys. Rev. B*, **76**(7), 075131. https://doi.org/10.1103/PhysRevB.76.075131.

Harrison, W.A. (2004), *Elementary Electronic Structure: Revised*, World Scientific Publishing Company, Singapore. https://doi.org/10.1142/5432.

Iordanidou, K., Houssa, M., van den Broek, B., Pourtois, G., Afanas'ev, V. and Stesmans, A. (2016), "Impact of point defects on the electronic and transport properties of silicene nanoribbons", *J. Phys. Condens. Matter.*, **28**(3), 035302. https://doi.org/10.1088/0953-8984/28/3/035302.

Jiang, Q., Zhang, J., Ao, Z., Huang, H. and Wu, Y. (2018), "Tuneable electronic and magnetic properties of hybrid silicene/silicane nanoribbons induced by nitrogen doping", *Thin Solid Films*, **653** 126-135. https://doi.org/10.1016/j.tsf.2018.03.004.

Leong, C.H., Chuan, M.W., Wong, K.L., Najam, F., Yu, Y.S. and Tan, M.L.P. (2020), "Compact device modelling of interface trap charges with quantum capacitance in MoS_2-based field-effect transistors", *Semicond. Sci. Technol.*, **35**(4), 045023. https://doi.org/10.1088/1361-6641/ab74f2.

LeSar, R. (2013), *Introduction to Computational Materials Science: Fundamentals to Applications*, Cambridge University Press, UK. https://doi.org/10.1017/CBO9781139033398.

Lim, W.H., Hamzah, A., Ahmadi, M.T. and Ismail, R. (2017), "Band gap engineering of BC2N for nanoelectronic applications", *Superlattices Microstruct.*, **112**, 328-338. https://doi.org/10.1016/j.spmi.2017.09.040.

Lim, W.H., Hamzah, A., Ahmadi, M.T. and Ismail, R. (2018), "Performance analysis of one dimensional BC2N for nanoelectronics applications", *Physica E Low Dimens. Syst. Nanostruct.*, **102** 33-38. https://doi.org/10.1016/j.physe.2018.04.005.

Liu, C.C., Jiang, H. and Yao, Y. (2011), "Low-energy effective Hamiltonian involving spin-orbit coupling in silicene and two-dimensional germanium and tin", *Phys. Rev. B.*, **84**(19), 195430. https://doi.org/10.1103/PhysRevB.84.195430.

Liu, G., Wu, M., Ouyang, C. and Xu, B. (2012), "Strain-induced semimetal-metal transition in silicene", *EPL.*, **99**(1), 17010. https://doi.org/10.1209/0295-5075/99/17010.

Lopez-Bezanilla, A. (2014), "Substitutional doping widens silicene gap", *J. Phys. Chem. C*, **118**(32), 18788-18792. https://doi.org/10.1021/jp5060809.

Low, S. and Shon, Y.S. (2018), "Molecular interactions between pre-formed metal nanoparticles and graphene families", *Adv. Nano Res., Int. J.*, **6**(4), 357-375. https://doi.org/10.12989/anr.2018.6.4.357.

Mehdi Aghaei, S. and Calizo, I. (2015), "Band gap tuning of armchair silicene nanoribbons using periodic hexagonal holes", *J. Appl. Phys.*, **118**(10), 104304. https://doi.org/10.1063/1.4930139.

Menezes, M.G. and Capaz, R.B. (2018), "Tight binding parametrization of few-layer black phosphorus from first-principles calculations", *Comput, Mater, Sci.*, **143**, 411-417. https://doi.org/10.1016/j.commatsci.2017.11.039.

Molle, A., Grazianetti, C., Tao, L., Taneja, D., Alam, M.H. and Akinwande, D. (2018), "Silicene, silicene derivatives, and their device applications", *Chem. Soc. Rev.*, **47**(16), 6370-6387. https://doi.org/10.1039/c8cs00338f.

Najam, F., Lau, K.C., Lim, C.S., Yu, Y.S. and Tan, M.L.P. (2016), "Metal oxide-graphene field-effect transistor: interface trap density extraction model", *Beilstein J. Nanotechnol.*, **7**(1), 1368-1376. https://doi.org/10.3762/bjnano.7.128.

Ni, Z., Zhong, H., Jiang, X., Quhe, R., Luo, G., Wang, Y., Ye, M., Yang, J., Shi, J. and Lu, J. (2014), "Tunable band gap and doping type in silicene by surface adsorption: towards tunneling transistors", *Nanoscale*, **6**(13), 7609-7618. https://doi.org/10.1039/c4nr00028e.

Novoselov, K.S., Geim, A.K., Morozov, S.V., Jiang, D., Zhang, Y., Dubonos, S.V., Grigorieva, I.V. and Firsov, A.A. (2004), "Electric field effect in atomically thin carbon films", *Science*, **306**(5696), 666-669. https://doi.org/10.1126/science.1102896.

Novoselov, K.S., Geim, A.K., Morozov, S., Jiang, D., Katsnelson, M.I., Grigorieva, I., Dubonos, S.V and Firsov, A.A. (2005), "Two-dimensional gas of massless Dirac fermions in graphene", *Nature*, **438**(7065), 197-200. https://doi.org/10.1038/nature04233.

Qin, R., Wang, C.H., Zhu, W. and Zhang, Y. (2012), "First-principles calculations of mechanical and electronic properties of silicene under strain", *AIP Adv.*, **2**(2), 022159. https://doi.org/10.1063/1.4732134.

Rodriguez-Perez, M., Villanueva-Cab, J. and Pal, U. (2017), "Evaluation of thermally and chemically reduced graphene oxide films as counter electrodes on dye-sensitized solar cells", *Adv. Nano Res., Int. J.*, **5**(3), 231-244. https://doi.org/10.12989/anr.2017.5.3.231.

Roome, N.J. and Carey, J.D. (2014), "Beyond graphene: stable elemental monolayers of silicene and germanene", *ACS Appl. Mater. Interfaces*, **6**(10), 7743-7750. https://doi.org/10.1021/am501022x.

Shao, Z.G., Ye, X.S., Yang, L. and Wang, C.L. (2013), "First-principles calculation of intrinsic carrier mobility of silicene", *J. Appl. Phys.*, **114**(9), 093712. https://doi.org/10.1063/1.4820526.

Song, Y.L., Zhang, Y., Zhang, J.M., Lu, D.B. and Xu, K.W. (2011), "First-principles study of the structural and electronic properties of armchair silicene nanoribbons with vacancies", *J. Mol. Struct.*, **990**(1-3), 75-78. https://doi.org/10.1016/j.molstruc.2011.01.020.

Takeda, K. and Shiraishi, K. (1994), "Theoretical possibility of stage corrugation in Si and Ge analogs of graphite", *Phys. Rev. B*, **50**(20), 14916. https://doi.org/10.1103/PhysRevB.50.14916.

Tao, L., Cinquanta, E., Chiappe, D., Grazianetti, C., Fanciulli, M., Dubey, M., Molle, A. and Akinwande, D. (2015), "Silicene field-effect transistors operating at room temperature", *Nat. Nanotechnol.*, **10**(3), 227-231. https://doi.org/10.1038/NNANO.2014.325.

Waldrop, M.M. (2016), "More than Moore", *Nature*, **530**(7589), 144-148. https://doi.org/10.1038/530144a.

Wang, Q.H., Kalantar-Zadeh, K., Kis, A., Coleman, J.N. and Strano, M.S. (2012), "Electronics and optoelectronics of two-dimensional transition metal dichalcogenides", *Nat. Nanotechnol.*, **7**(11), 699-712. https://doi.org/10.1038/NNANO.2012.193.

Wang, Y., Huang, R., Kong, F., Gao, B., Li, G., Liang, F. and Hu, G. (2019), "Tunable electronic and optical properties of the $MoS_2/MoSe_2$ heterostructure nanotubes", *Superlattices Microstruct.*, **132**, 106156. https://doi.org/10.1016/j.spmi.2019.106156.

Watts, M.C., Picco, L., Russell-Pavier, F.S., Cullen, P.L., Miller, T.S., Bartuś, S.P., Payton, O.D., Skipper, N.T., Tileli, V. and Howard, C.A. (2019), "Production of phosphorene nanoribbons", *Nature*, **568**(7751), 216-220. https://doi.org/10.1038/s41586-019-1074-x.

Wong, K.L., Chuan, M.W., Alias, N.E., Hamzah, A., Lim, C.S. and Tan, M.L.P. (2019), "Modeling of low-dimensional pristine and vacancy incorporated graphene nanoribbons using tight binding model and their electronic structures", *Adv. Nano Res., Int. J.*, **7**(3), 209-221. https://doi.org/10.12989/anr.2019.7.3.209.

Wong, K.L., Chuan, M.W., Hamzah, A., Rusli, S., Alias, N.E., Sultan, S.M., Lim, C.S. and Tan, M.L.P. (2020), "Performance metrics of current transport in pristine graphene nanoribbon field effect transistors using recursive non-equilibrium Green's function approach", *Superlattices Microstruct.*, **145**, 106624. https://doi.org/10.1016/j.spmi.2020.106624.

Yang, C., Yu, Z., Lu, P., Liu, Y., Ye, H. and Gao, T. (2014), "Phonon instability and ideal strength of silicene under tension", *Comput. Mater. Sci.*, **95**, 420-428. https://doi.org/10.1016/j.commatsci.2014.07.046.

Xue, P., Chen, A., Zhang, J. and Shao, Q. (2019), "Transport properties of doped zigzag graphene nanoribbons", *Chinese J. Phys.*, **57**, 47-52. https://doi.org/10.1016/j.cjph.2018.12.014.

Yang, X. and Ni, J. (2005), "Electronic properties of single-walled silicon nanotubes compared to carbon nanotubes", *Phys. Rev. B.* **72**(19), 195426. https://doi.org/10.1103/PhysRevB.72.195426.

Ye, P., Ernst, T. and Khare, M.V. (2019), "The last silicon transistor: Nanosheet devices could be the final evolutionary step for Moore's law", *IEEE Spectrum*, **56**(8), 30-35. https://doi.org/10.1109/MSPEC.2019.8784120.

Zhang, J.M., Song, W.T., Xu, K.W. and Ji, V. (2014), "The study of the P doped silicene nanoribbons with first-principles", *Comput. Mater. Sci.*, **95**, 429-434. https://doi.org/10.1016/j.commatsci.2014.08.019.

Zhao, J., Liu, H., Yu, Z., Quhe, R., Zhou, S., Wang, Y., Liu, C.C., Zhong, H., Han, N. and Lu, J. (2016), "Rise of silicene: a competitive 2D material", *Prog. Mater. Sci.*, **83**, 24-151. https://doi.org/10.1016/j.pmatsci.2016.04.001.

CC